Pro-Gly Mediated Conformational Switch of Mycobacteriophage D29 Holin Transmembrane Domain I is Lipid Concentration Driven

Muralikrishna Lella and Radhakrishnan Mahalakshmi[a]*

[a] Molecular Biophysics Laboratory, Department of Biological Sciences, Indian Institute of Science Education and Research, India.

Electronic Supplementary Information

Contents:

EXPERIMENTAL SECTION

Reagents and Chemicals:

All reagents and chemicals used for the synthesis including LDAO (Lauryldimethylamine N-oxide) were obtained in their purified form from Sigma-Aldrich Co. LLC and used without further purification. Rink amide AM resin (loading capacity of 0.63meq, 200-400 mesh) was purchased from Novabiochem (EMD Millipore Chemicals). Fmoc protected amino acids and HATU ((Dimethylamino)-N,N-dimethyl (3H-[1,2,3]triazolo [4,5-b] pyridin-3-yloxy) methaniminium hexafluorophosphate) were purchased from GL Biochem Shanghai Ltd., and were supplied as >98-100% pure. Other buffers, reagents for peptide synthesis and cleavage cocktail were purchased from Sigma-Aldrich Co. LLC. Diethyl ether was obtained from Merck Specialties Pvt. Ltd. All lipids and detergents were obtained from Avanti Polar Lipids, Inc. SYPRO® Orange was obtained from Invitrogen (Life Technologies Corporation).

Peptide Synthesis:

Peptides were synthesized by standard solid phase synthesis on a Rink Amide AM resin using Fmoc chemistry. Fmoc deprotection was achieved using 20% piperidine prepared in dry DMF, and carboxyl group activation was achieved using a mixture of HATU and DIPEA (N,N-ethyldiisopropylamine) (Hünig's base) in dry DMF (dimethylformamide). Three equivalents were used for each coupling and the progress of the reaction was monitored by Kaiser test. Each coupling was repeated at least twice to achieve saturation of all reaction sites. Unreacted sites were not blocked before proceeding to the next amino acid. Progress of the reaction was also monitored using mass spectrometric analysis on a micrOTOF-Q II mass spectrometer (Bruker Daltonik GmbH) in methanol. After completion of the synthesis, Fmoc group was deprotected to generate a free N-terminus. DMF was then removed using diethyl ether washes and the resin was air-dried. The peptide was simultaneously side-chain deprotected and cleaved from the resin using the following cleavage cocktail: TFA (82.5) : water (5.0) : phenol (5.0) : thioanisole (5.0) : ethanedithiol (2.5). 1ml of this cleavage cocktail was used to deprotect 1mg of dried resin. The cleavage reaction was allowed to proceed for at least 12h at 25°C. After completion of the cleavage reaction, the resin was filtered off and peptide was precipitated using diethyl ether. The peptide was repeatedly washed with cold diethyl ether to remove residual cleavage cocktail reagents. The peptide was recovered by centrifugation for 30min at 4°C at 50,000 x g, and finally air dried. The sequences described in this study are listed below with their calculated (using http://www.peptidesynthetics.co.uk/tools/) and observed molecular weights (described below):

Peptide Code	Peptide Sequence	Monoisotopic MW	
		Calculated	Observed (M+H⁺)
TM1	H$_3$N-KIRETLYYVGTLV**PG**ILGIALIWGGIDA-CONH$_2$	2999.711Da	3001.214
TM1:A	H$_3$N-KIRETLYYVGTLV**AA**ILGIALIWGGIDA-CONH2	2987.711Da	2989.064
TM1:^{D}P	H$_3$N-KIRETLYYVGTLV^D**PG**ILGIALIWGGIDA-CONH$_2$	2999.711Da	2999.959

Peptide Purification and Mass Spectrometric Analysis:

The final peptides exhibited poor solubility in various solvents tested, including acetonitrile, water, methanol and isopropanol, owing to the presence of several hydrophobic amino acids. The peptides exhibited solubility in detergent-containing solutions and in TFE (trifluoroethanol), which were not conducive for purification. Hence, all samples were extensively washed with diethyl ether to remove small molecule impurities from the cleavage reaction and used without subsequent purification. Sample homogeneity and absence of any deletions were confirmed using mass spectrometry. MALDI spectra

were acquired on an UltrafleXtreme MALDI-ToF/ToF mass spectrometer (Bruker Daltonik GmbH) using HCCA (α-cyano-4-hydroxycinnamic acid) matrix prepared in 50% acetonitrile containing 0.1% TFA. ESI data was obtained on a micrOTOF-Q II platform (Bruker Daltonik GmbH) using acetonitrile containing 1% acetic acid as the mobile phase.
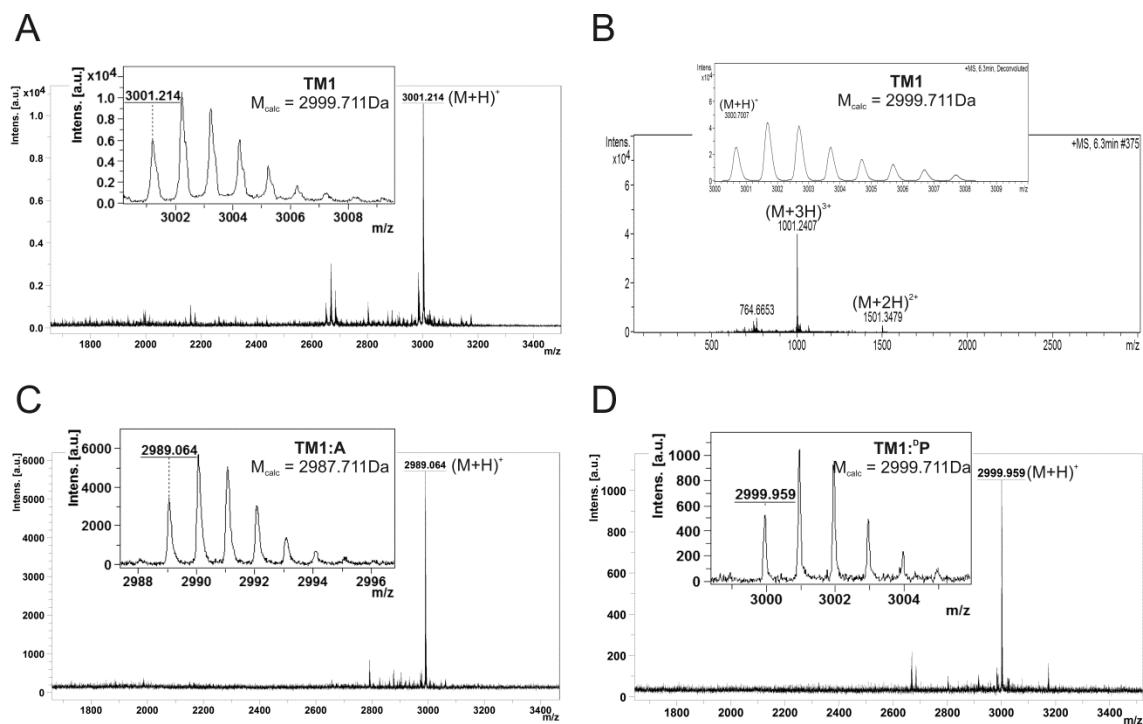
Mass spectra of all the peptides are shown above. MALDI-ToF (A) and ESI (B) mass spectra of D29 holin **TM1**, MALDI-ToF spectra of **TM1:A** (C) and **TM1:**^D**P** (D) are shown with insets highlighting the isotopic distribution observed for each peptide. The calculated mass and the observed charge distribution are also indicated in each spectrum.

Peptide Refolding

Peptide refolding was attempted in a wide variety of detergents and lipids. Detergents such as LDAO and SDS (sodium dodecyl sulfate) were supplied as powders and were weighed directly. For preparation of lipids and detergents that were available in the chloroform solubilized state, aliquots of the required concentrations were first evaporated on a centrifugal concentrator to remove chloroform, followed by brief lyophilization. All lipids and detergents were re-suspended in 50mM sodium phosphate buffer, pH 7.2 (stock preparations: 100mM LDAO, 50mM DPC (*n*-dodecylphosphocholine), 200mM 6OPC (1,2-di-O-hexyl-*sn*-glycero-3-phosphocholine), 160mM SDS.Peptide powder was directly added to the various lipid stocks and the mixture was subjected to multiple cycles of vortexing, heating to ~45-50°C and sonication. Undissolved material, if any, was removed by centrifugation. Samples thus prepared served as the stock refolded peptide, which was diluted to an A_{295} = 0.1 using phosphate buffer (with or without lipid) for all experiments. Final samples so prepared contained 0.022-0.024mM peptide in the desired concentration of lipid or detergent.

Direct peptide refolding in the final lipid concentrations were also attempted, wherein the peptide powder was directly mixed with the required lipid prepared in 50mM phosphate buffer pH 7.2, and this sample was subjected to cycles of vortexing, sonication and heating, to completely dissolve the peptide. All samples were subjected to high speed centrifugation to remove particulate material. Samples were

then quantified and peptide concentrations were adjusted to ~0.022-0.024mM, as before, wherever necessary.

NMR Experiments:

^{1}H 1D experiments were recorded on a Bruker Avance III 700MHz instrument (Bruker BioSpin GmbH) at 298K. The final NMR sample contained 1.2mM peptide and 200mM LDAO in 50mM sodium phosphate buffer pH 7.2 containing 10% D_2O. Higher peptide concentrations required for NMR experiments could not be readily achieved without increasing LDAO amounts; the latter led to substantial line broadening due to unfavorable τ_c values of these highly viscous preparations. Samples were also prepared in TFE containing 6% DMSO-d_6; here the highest peptide concentration that could be achieved was 1.66mM. All spectra were acquired with water suppression using the pre-saturation *zgpr* pulse program available in the standard Bruker library, using 32K data points. 2000 scans were accumulated for the LDAO sample and 1000 scans for the TFE sample. Spectra in TFE were acquired with double pre-saturation (residual water and -CH_2- resonance of TFE). Data were processed with a 0.6Hz line broadening and plots were generated using Topspin v3.0 (Bruker BioSpin GmbH). Referencing was achieved with using water chemical shift at 298K. Spectra obtained are provided below.
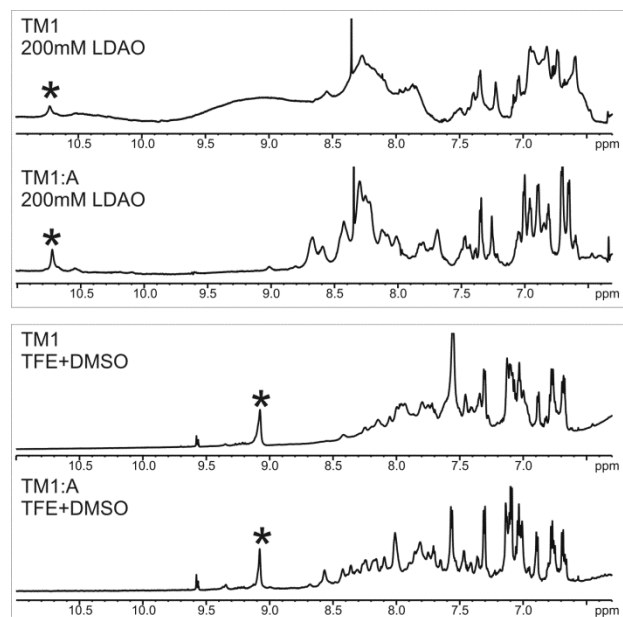
Shown is the expansion of the amide region of the spectrum. Significant contribution from LDAO was observed below 5.0ppm, which masked other resonances from the peptide. Extensive line broadening was observed in all cases, especially the LDAO-containing samples, due to the slow tumbling rates of micellar samples. In TFE, while the peptide was soluble in low concentrations, addition of DMSO was required to obtain the concentrations necessary to achieve acceptable S/N in the NMR spectrum. The LPR used for the peptide refolded in 200mM LDAO here is ~166:1. Under these conditions, it is anticipated that **TM1** adopts a sheet-like structure, while **TM1:A** is helical. Since **TM1:A** can adopt better structure compared to **TM1**, marginally better S/N and line widths are observed for this peptide. The indole amide resonance is indicated by '∗'. Downfield shifted N$^{\varepsilon 1}$H resonance in LDAO samples indicates that the Trp residue is shielded from the solvent and is in a well-folded conformation, which is expected if the peptide is embedded in lipid micelles.

Circular Dichroism Experiments:

All circular dichroism (CD) measurements were carried out on a JASCO J815 CD spectropolarimeter (Jasco Inc., Japan) equipped with a 450W Xe lamp and water cooled peltier temperature control unit. Sample concentrations were adjusted to 0.022-0.024mM, which corresponded to an A_{295} = 0.1. This allowed us to directly correlate the CD data with that of fluorescence measurements, without changing peptide and lipid concentrations. Far-UV CD spectra (wavelength scans) were recorded using a 1mm path length quartz cell with 0.5 or 1nm band width, 1s data integration time and 100nm/min scan speeds. Data were averaged over at least three accumulations, blank subtracted and smoothened. For dilution experiments, spectra were recorded in cuvettes of various path

lengths from 1mm to 10mm, so as to obtain a good signal-to-noise for the dilute samples. Other parameters were maintained as described above.

Thermal denaturation measurements were recorded between 5°C-95°C for samples prepared in aqueous media. Effective ramp rates of 1°C/min were used and wavelength scans (as described above) were acquired, at increments of every 5°C. Recovery from thermal denaturation was also monitored using the same parameters, while the sample was cooled from 95°C-5°C. Data processing was carried out using Spectra Manager v2.0 (Jasco Inc.). All spectra were blank subtracted and converted to molar ellipticity (*ME*) values using the formula:

$$ME = \frac{\theta}{10 \; x \; c \; x \; l}$$

where, θ is the observed ellipticity in millidegrees, c is the peptide concentration in molarity and l is the path length in centimeters. The final data were plotted using SigmaPlot v11.0 (Systat Software, Inc.).

Steady State Fluorescence, Anisotropy and Lifetime Measurements:

Steady state fluorescence and anisotropy measurements were carried out on a FluoroMax-4 spectrofluorometer (Horiba Jobin-Yvon, France) equipped with air-cooled peltier control. Both excitation and emission slit widths were set at 3nm for steady state fluorescence measurements and 5nm for anisotropy experiments. Excitation wavelength was fixed at 295nm and emission spectra were recorded between 310nm and 400nm using a step size of 0.5nm and data integration time of 0.1s. Emission wavelength was additionally set at 345nm for the anisotropy measurements for and an integration time of 5s was used. Sample concentrations were maintained at ~0.022-0.024mM using A_{280} values and calculated molar extinction coefficient of 8480 M^{-1} cm^{-1}, which thereby gave an A_{295} = 0.1, optimal for all fluorescence experiments. All spectra were blank subtracted and corrected for dark counts. All experiments were repeated multiple times using independent sample preparations, to check for data reproducibility.

Fluorescence lifetime measurements were carried out on a FluoroLog spectrofluorometer (Horiba Jobin-Yvon, France) using TCSPC (time-correlated single photon counting). Excitation maximum was set at 295nm and the decay was recorded at magic angle of 54.7° and monitored at either 345nm or 347nm for LDAO and DPC samples, respectively, at 355nm for sample in 50mM phosphate buffer. These wavelengths corresponded to the emission maxima in steady state tryptophan fluorescence measurements of both peptides in the respective sample conditions. Skimmed milk was used to monitor the instrument response function (IRF), which was ~815ps in most experiments. Lifetime values and corresponding amplitude fractions, as well as average lifetimes, were derived using fits of data to a triple exponential decay function using the DAS6 v6.4 software. Plots were generated using SigmaPlot v11.0.

Thioflavin T and SYPRO Orange Assay:

Thioflavin T (ThT) and SYPRO® Orange assays were monitored on the FluoroMax-4 spectrofluorometer. ThT assays were carried out using reported protocols.[1] Briefly, 10µM ThT, dissolved in 50mM phosphate buffer pH 7.2, was added to 200µl of peptide (~0.022-0.024mM), and the sample was incubated at 25°C for 30min to allow ThT binding to peptide. Samples were excited at 450nm and the emission spectra were recorded between 465nm to 550nm using a 0.5nm increment. Excitation and emission slit widths were set at 5nm and a 0.1s data integration time was used.

For SYPRO® Orange assays, peptide concentrations were maintained at ~0.022-0.024mM and a SYPRO® Orange was added to the sample to achieve a final concentration of 10X dye (from a 5000X stock, as supplied by the manufacturer; manufacturer instructions were followed for dye preparation). Assays were carried out using reported protocols.[2] Samples were excited at 480nm and emission spectra were recorded from 550nm to 650nm, using an increment step of 0.5nm. Data integration time was set at 0.1sec and emission and excitation slit widths were set at 2nm and 4nm respectively.

All samples in both experiments were subtracted with the respective blanks and plotted using SigmaPlot v11.0. Spectra obtained for the ThT assays to detect amyloid formation, are shown below.
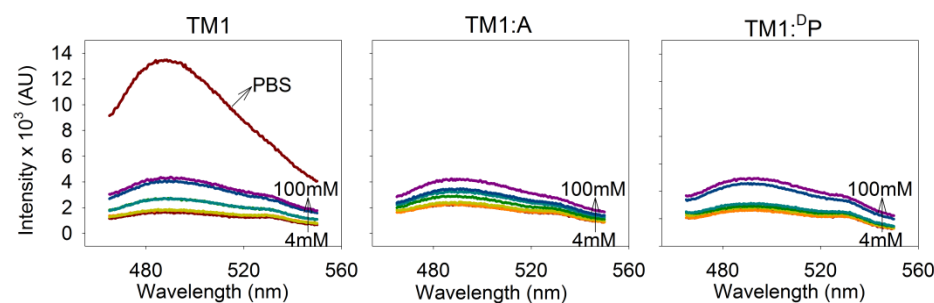
ThT exhibits a characteristic increase in fluorescence intensity upon binding to ordered β-sheets of the kind usually observed in amyloid-like structures.[1] In both **TM1** (left) and **TM1:A** (middle) and **TM1:^{D}P** (right) in LDAO micelles of various concentrations (4-100mM), addition of ThT to the refolded peptide samples only causes a marginal increase in fluorescence, which could be attributed to differential interaction affinity for the fluorophore to the protein-lipid complex. However, in the absence of any lipid medium for peptide folding, soluble aggregates are formed (PBS). When added to these aggregates, ThT shows a nearly 3.5-fold increase in fluorescence intensity (spectrum marked as PBS), compared with the highest fluorescence obtained for refolded **TM1** (left). Baseline fluorescence is also observed in **TM1:A** (middle), in the refolded peptides. It is particularly notable that **TM1** refolded in 4mM LDAO shows CD spectra characteristic of a β-sheet like structure. This could arguably arise also due to peptide aggregation. However, our data indicates that ThT does not bind to peptide in 4mM LDAO, indicating that the peptide is not in an aggregated form in solution. As the sample in 4mM LDAO shows negligible ThT fluorescence, it indicates that **TM1** in low LPR indeed adopts a β-sheet structure and is embedded in lipid micelles. Similarly, in the case of **TM1:^{D}P** (right), which adopts a β-sheet structure in all tested lipid conditions, substantial increase in ThT fluorescence to levels comparable to peptide in buffer (indicated as PBS in the left spectrum), is not observed. This suggests that **TM1:^{D}P** is also enveloped by lipid micelles and is not in an aggregated form, despite adopting a β-sheet structure.

Structure Simulation:

Structure prediction of all sequences was carried out using the I-TASSER server.[3] Prediction was carried out using the default parameters without any additional restraints; templates were neither included nor excluded during the prediction. 3D models that were generated were rendered using PyMOL (Schrödinger, LLC).[4] The structures are shown below.

Planar Bilayer (Black Lipid Membrane; BLM) Experiments:

Planar lipid bilayers were prepared by painting lipid onto a 150µm aperture in the septum of a Delrin cup. The lipid, DPhPC (diphytanoyl phosphatidylcholine), was dissolved in *n*-hexadecane at 50mg/ml. A working volume of 1ml sodium phosphate buffer 7.2 pH containing 500mM KCl was maintained on both the *cis* and *trans* sides of the chamber, and was separated by the bilayer. A bilayer thickness corresponding to a capacitance of 35pF was achieved for all experiments. 0.057mM peptide in 100mM LDAO was added to the *cis* side of the chamber at a set voltage of 0mV. Insertion of **TM1** was achieved when the voltage was ramped to 30mV. The electrical current was recorded using Bilayer Clamp BC535 amplifier (Warner Instruments, Harvard Apparatus, MA) and data were filtered at 50Hz with low pass 8-pole bessel filter and the output was digitized using Digidata1440A (Molecular Devices LLC (Axon Instruments)) using a sampling frequency of 10kHz. The chamber was placed in a Faraday cage set on a mechanically isolated table, in order to minimize electrostatic interference and obtain low-noise recording. All data were analyzed using the pCLAMP 10.3 software (Molecular Devices) and plotted using SigmaPlot.

SUPPLEMENTARY FIGURES
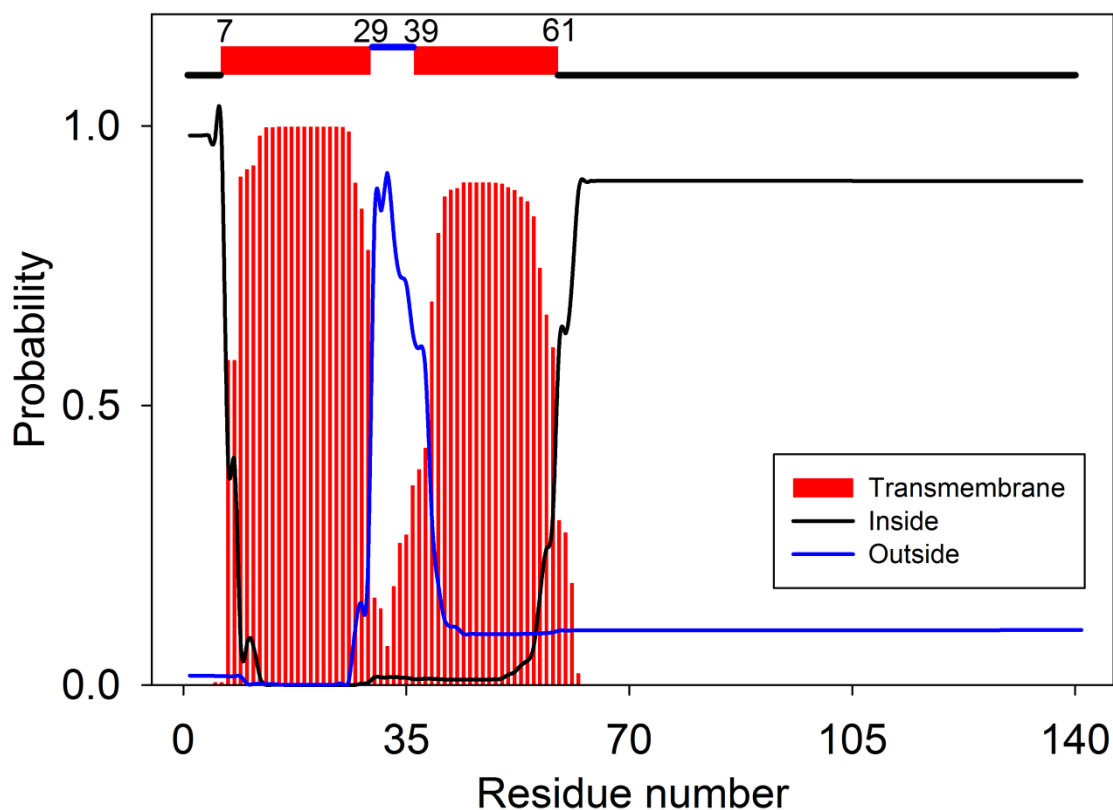
Figure S1. Prediction of the transmembrane regions of D29 holin. Potential transmembrane region of full-length D29 holin was generated using TMHMM v2.0.[5] Scores generated for the orientation and occupancy in the transmembrane region was plotted using SigmaPlot v 11.0. Here, probability of occurrence in the transmembrane region is plotted against residue number. The predicted transmembrane region is represented as red. Probability of orientation of the extra-membrane regions of the protein is given as solid black (inside, towards cytosol) or solid blue (outside, towards inter-membrane space) lines. Also indicated above the prediction is the schematic representation of the protein with the start and end residues for the various segments. Residues 7-29 are presumed to constitute the first transmembrane segment, while the second transmembrane region is comprised of residues 39-61.

```
D29          MSPKIRETLYYVGTLVPGILGIALIWGGIDAGAAANIGDIVAGALNLVGAAAPATAAVKV 60
DaVinci      MNPKVRQSLYYVGTIVPGVLGIALLWGGIDAGAADNIGLVVSGVLNILGASAPATAAVTV 60
Gladiator    MNPKVRQSLYYVGTIVPGVLGIALLWGGIDAGAADNIGLVVSGVLNILGASAPATAAVTV 60
EricB        MNPQVRQTLYYLGTIVPGVLGIALIWGGIDAGAANNIGLIVSGALNILGAGAPATAAVTI 60
SWU1         MSPKIRQTIYLLGTAAPALLGIVLIWGGLDAESAADLGDIIAGVVSLLVSGAPAVAAGTV 60
L5           MSPKIRQTIYLLGTAAPALLGIVLIWGGLDAESAADLGDIIAGVVSILVSGAPAVAAGTV 60
LHTSCC       MSPKIRESLYYVGTIIPALLGLGMIWGGIDAGAASSIGDILAGALALIGATAPATAAVKV 60
Pukovnik     MSPKIRETLYYVGAIVPALLGIALIWGGIDAGAADSIGSIIAGALNLIGATAPAVAAKKV 60
Peaches      MSPKVRQTIYYLGTIIPGVLGIALIWGGIDAGAAQSIGDIIAGAVALLGASAPAVAAKKV 60
ToriTheta9   MSPKVRQTIYYLGTIIPGVLGIALIWGGIDAGAAQSIGDIIAGAVALLGASAPAVAAKKV 60
Backyardigan MSPKIRESLYYVGTIIPALLGLGMIWGGIDAGAAESIGSIVTGALALLGAVAPATAAVKV 60
First        MSPKVRQSIYHVGTLIPGLVGLAMIWFGLSTDDADSIIQVVSGAIALIGAGAPAIAAKTV 60
Turbido      MSPKIRQSIYHVGTLIPGLVGLAMLWFGLSSDDADSIIQVISGALALIGAGAPAIAAKTV 60
             *.*::*:::* :*: *.::*: ::* *:.:  *  .:  :::*.: :: : *** **  .:

D29          NQQRKDGTLT-TSPVDQVTRGVEQVLAAKQNAEAEVERVKQALESAV-----NGAVPQLG 114
DaVinci      GKQRKDGTLT-GSPVESVVKGVEQVLAAQQTAQAEVEQVRQAIESAV-----TGAVPALG 114
Gladiator    GKQRKDGTLT-GSPVESVVKGVEQVLAAQQTAQDEVEQVRQAIESAV-----TGAVPALG 114
EricB        SKQRKDGTLT-GSPVESVVKGVEQVLAAHQAAQEEVEQVRQAIESAV-----TGAVPALG 114
SWU1         RSQRKDGTLS-TSPVDQVTKGVEQVLAARQSAEAEVAKVKQALETAV-----SGSLPQLG 114
L5           RSQRKDGTLS-TSPVDQVTKGVEQVLAARQSAEAEVAKVKQALETAV-----SGSLPQLG 114
LHTSCC       NKQRKDGTLEPLAPVDQVVNGVQAVIAAQHAAQAELDRVKDAVTGAIG--VIPGVLPQLG 118
Pukovnik     NEQRKDGTLS-ASPVDAVVKGVEQVVAARNAAQAEVEKVTQVVGGVLSDVQRAAEAVNLG 119
Peaches      NEQRKDGTLVPQAPVEQVVNGVQAVIAAQQAAQAELDRVRDVVTGAIG--IVPGIVPQLG 118
ToriTheta9   NEQRKDGTLVPQAPVEQVVNGVQAVIAAQQAAQAELDRVRDVVTGAIG--IVPGIVPQLG 118
Backyardigan NQQRKDGTLEPIAPVEQVVNGVQAVIAAQQAAQAELDRVKDAVTGAIG--IVPNIVPQLG 118
First        REQRKDGTLT-ANPVEAVSKGIEQVIAARDAAQAEVDKVTSVVGNVLSDVQLAANAINLG 119
Turbido      RDQRKDGTLT-ASPVEAVSKGIEQVIAARDAAQAEVEKVTSVVGNVLNDVQLAANAVNLG 119
              .*******    **:  *  .*:: *:**:. *: *: :*  ..:   .:         **

D29          PLASQ---------ILNGIQP--AYS---QPFDPHTQPWNR- 141
DaVinci      PLAQQ---------VINSVVPQQAYS---QLYDPNTQPWNR- 143
Gladiator    PLAQQ---------VINSVVPQQAYS---QLYDPNTQPWNR- 143
EricB        PLAQQ---------VINSVVPQQAYS---QLYDPNTHPWNRG 144
SWU1         PLATQ---------ILN-VADDTVWR-----------P---- 131
L5           PLATQ---------ILN-VADDTVWR-----------P---- 131
LHTSCC       PLAQQAVD------AVN--AFPTAYSQVPQFTD-YRQPWDR- 150
Pukovnik     PLASQILNGLPNGFAPRAFAPHQAYS-QAYDYDPVTLPQIR- 159
Peaches      PLAQQAVD------ALNGFAPPTAYSQAAQFADPYRAPWDR- 153
ToriTheta9   PLAQQAVD------ALNSFAPPTAYSQAAQFADPYRAPWDR- 153
Backyardigan PLAQQAVD------AINGFAPPTAYSQAAQYVDPYRAPYDR- 153
First        PLASQILNG------AQDALSPQAYS-LYDPTTAWRRPEDR- 153
Turbido      PLASQILSAL-----PVDHQPPTAYS-LYDPNNSWRRPEDR- 154
             *** *                     .:            *
```

Figure S2. Multiple sequence alignment of some representative holins of various mycobacteriophages. Full-length D29 holin was aligned using standard parameters of ClustalW2 (http://www.ebi.ac.uk/Tools/msa/clustalw2/). Standard amino acid color codes, as provided by ClustalW2, are shown here. The PG segment of TM1 is boxed. Note the conserved substitution to PA in some holins from related mycobacteriophages.

Figure S3. Amino acid propensities of the predicted transmembrane domains of D29 holin. Propensities of various amino acids for the two secondary structural elements, namely, β-sheets (black bars) and α-helix (grey bars), obtained from the Biological Magnetic Resonance Bank (BMRB)[6] are plotted for the first transmembrane domain (A), which corresponds to **TM1**, and sequence of the second transmembrane domain (B). Residues that are proposed to adopt an extended structure upon conformational conversion of **TM1** are highlighted in red. Also shown are the relative propensities of each residue to be found in sheets, calculated as P_β-P_α, where P_β and P_α are the absolute propensities of any residue to occur in a β-sheet or α-helix, respectively. Note the general propensity for most residues to occur in extended structures, in the first transmembrane region (A). On the contrary, note that most residues show large negative values in the second transmembrane region (B), indicating that residues in this unit intrinsically prefer adopting a helical conformation.
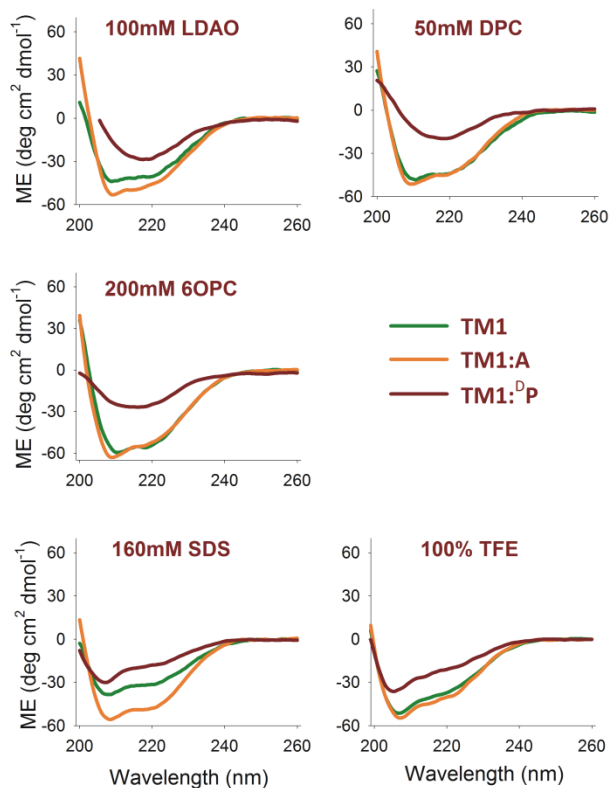
Figure S4. Representative far-UV CD spectra of the three peptides **TM1**, **TM1:A** and **TM1:^{D}P**, refolded in various lipids, detergents and solvents. All lipids and detergents were prepared in 50mM sodium phosphate buffer pH 7.2. Both **TM1** and **TM1:A** exhibit CD spectra corresponding to a helical structure, with negative maxima at ~208nm and 222nm in all the conditions illustrated here. However, **TM1:^{D}P** shows a helical CD spectrum only in SDS and TFE, since both these media are known to induce helical structures in short peptides. Furthermore, **TM1:^{D}P** displays a signature β-sheet CD spectrum, which is a broad trough with a negative maximum centered at ~215nm, in membrane mimetic environments such as LDAO, DPC and 6OPC. In all spectra, ME (molar ellipticity) values are factored by 10^4.
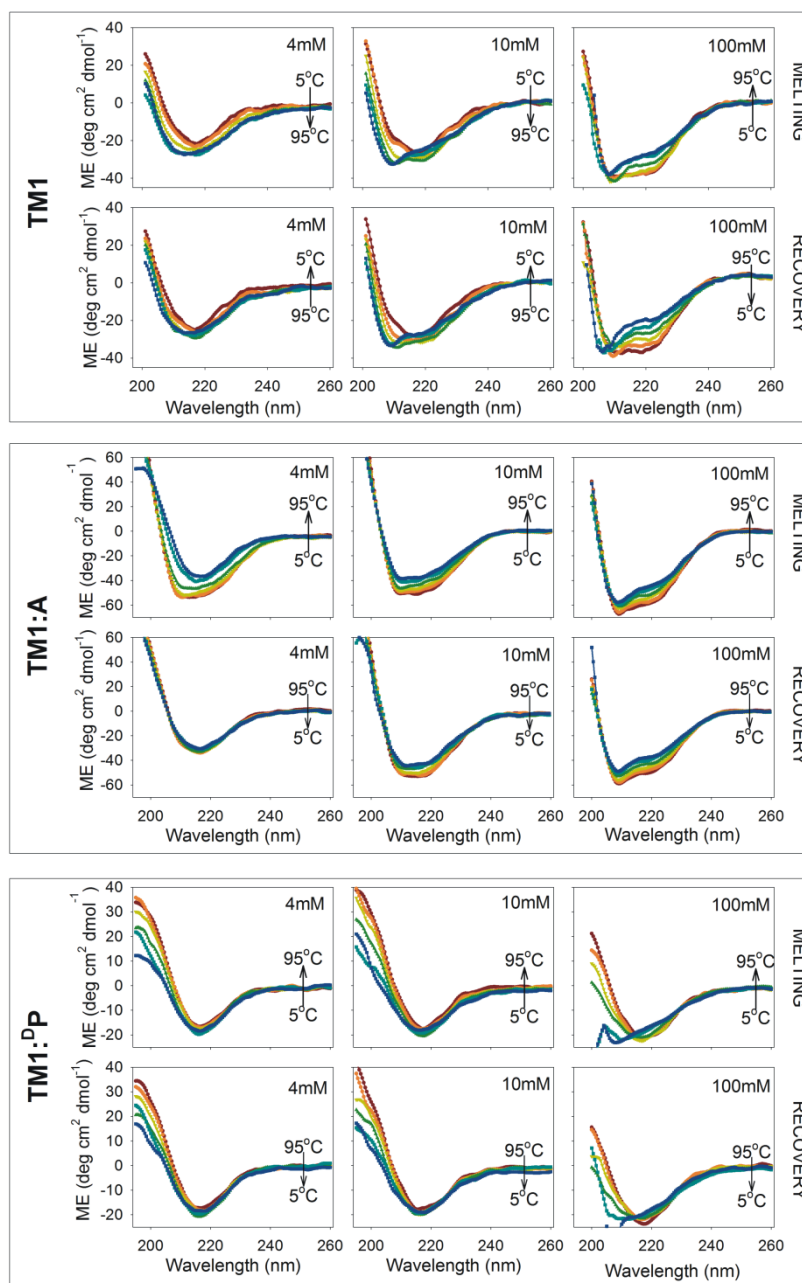
Figure S5. Representative thermal denaturation (melting) and recovery measurements in 4mM, 10mM and 100mM LDAO for **TM1** (top), **TM1:A** (middle) and **TM1:^{D}P** (bottom). All ME (molar ellipticity) values are factored by 10^4. Note the conformational interconversion of **TM1** at low LPRs of 4mM and 10mM LDAO upon heating, occurs through a helical intermediate, and is accompanied by an increase in molar ellipticity. On the contrary, **TM1:^{D}P** does not exhibit a similar profile. In 100mM LDAO, **TM1** displays a signature helical CD spectrum. At low LPRs, **TM1** closely resembles the spectroscopic properties of **TM1:^{D}P**. At high LPR, **TM1** displays CD properties that are similar to **TM1:A**. Furthermore, **TM1:A** undergoes irreversible denaturation in low LDAO (4mM) and requires higher micellar concentrations to exhibit thermal stability. In all cases, an ~2-3 fold higher CD (and corresponding ME) value is observed when the peptide adopts a helical conformation, in line with the greater ability of this structure to interact with left- versus right-circularly polarized light.
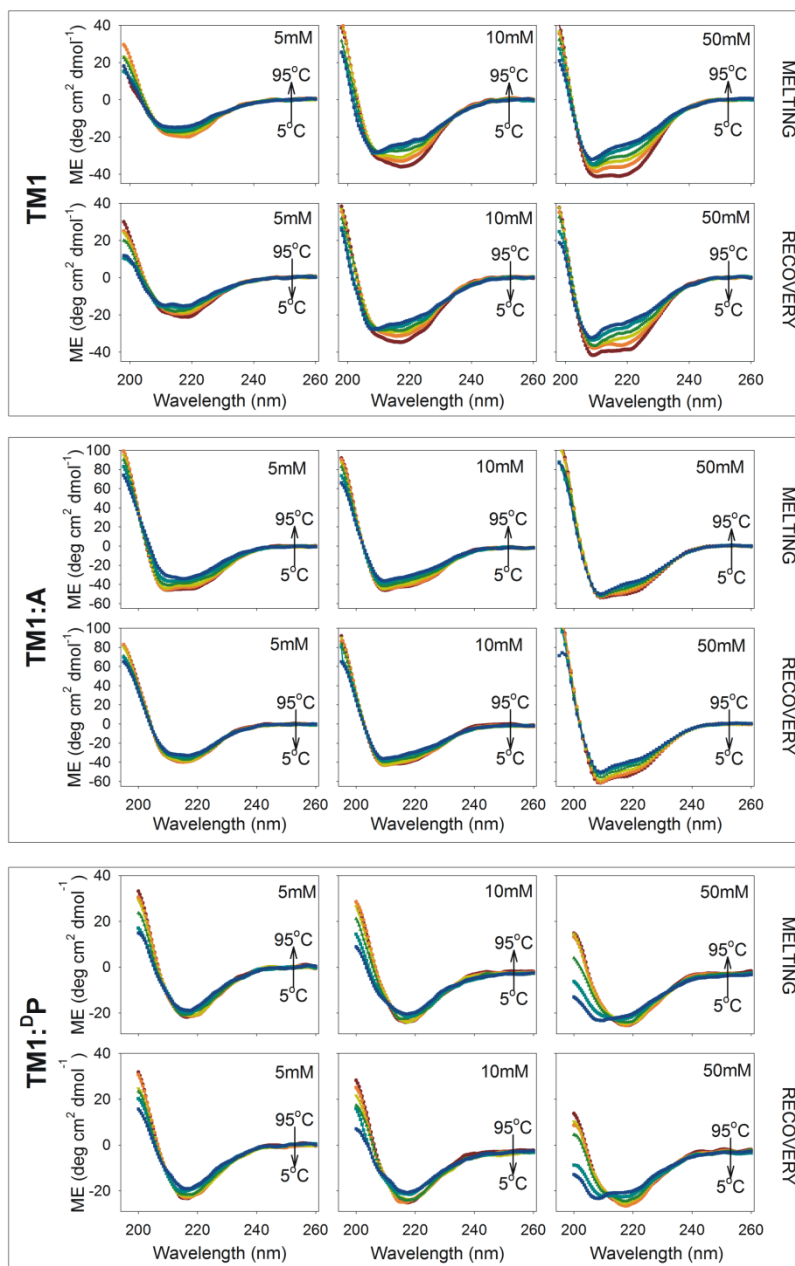
Figure S6. Representative thermal denaturation (melting) and recovery measurements in 5mM, 10mM and 50mM DPC for **TM1** (top), **TM1:A** (middle) and **TM1:^{D}P** (bottom). All ME (molar ellipticity) values are factored by 10^4. **TM1** undergoes a reversible conformational change to helix with increase in DPC as well as upon heat denaturation. Additionally, note that in 10mM DPC, **TM1** exhibits a CD spectrum characteristic of a mixed α+β population. **TM1:A** undergoes irreversible denaturation in 5mM DPC and stays helical in higher DPC amounts. **TM1:^{D}P** shows reversible unfolding upon heating, in 50mM DPC with a conversion to partially unfolded state at higher temperature. In all cases, an ~2-3 fold higher CD (and corresponding ME) value is observed when the peptide adopts a helical conformation, similar to that observed in LDAO.
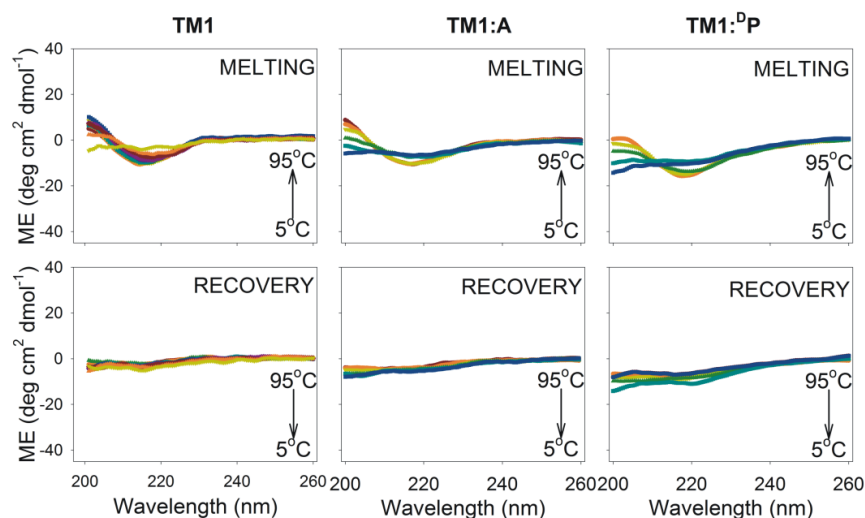
Figure S7. Control experiment, monitoring the melting and recovery of **TM1** (left) and **TM1:A** (middle) and **TM1:^{D}P** (right) in phosphate buffer in the absence of any lipid or detergent, wherein the peptide is expected to remain in the unfolded, and possibly aggregated form. Note the complete loss of structure and peptide aggregation upon heating, in all three peptides indicating that lipid environment is mandatory for its stability. Such observation is also seen for a few characterized transmembrane proteins of the β-barrel category.[7] ME (molar ellipticity) values are factored by 10^4.
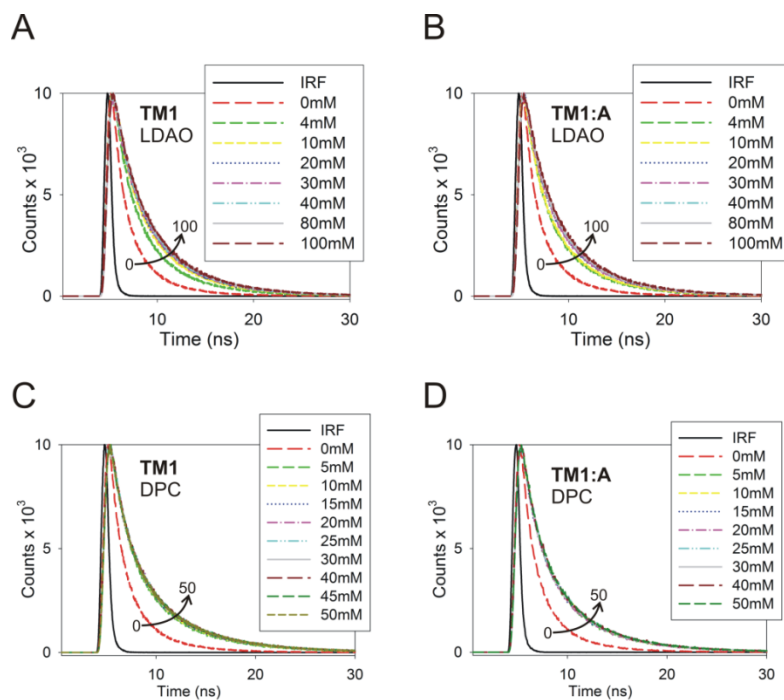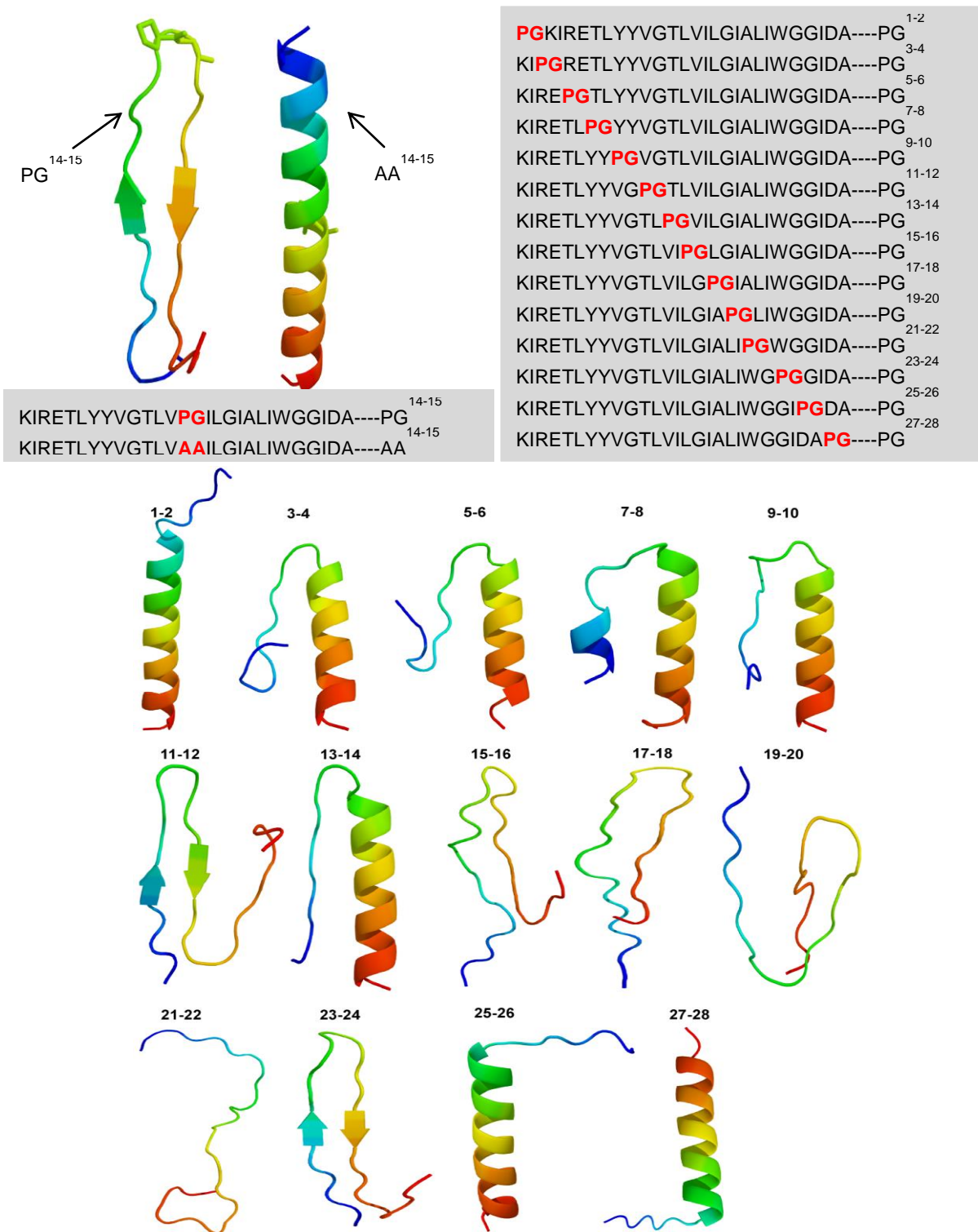

Figure S8. Representative decay profiles for fluorescence lifetime measurements. Fluorescence decay profiles of **TM1** with increasing LDAO (A) and DPC (B) concentrations, with aggregated peptide (peptide in buffer) indicated as 0mM. Decay profiles for **TM1:A** in LDAO (C) and DPC (D) are compared with aggregated peptide marked as 0mM. Note that the decay curves for the refolded peptide are dramatically different from the aggregated peptide in buffer. In all profiles, IRF refers to instrument response function.
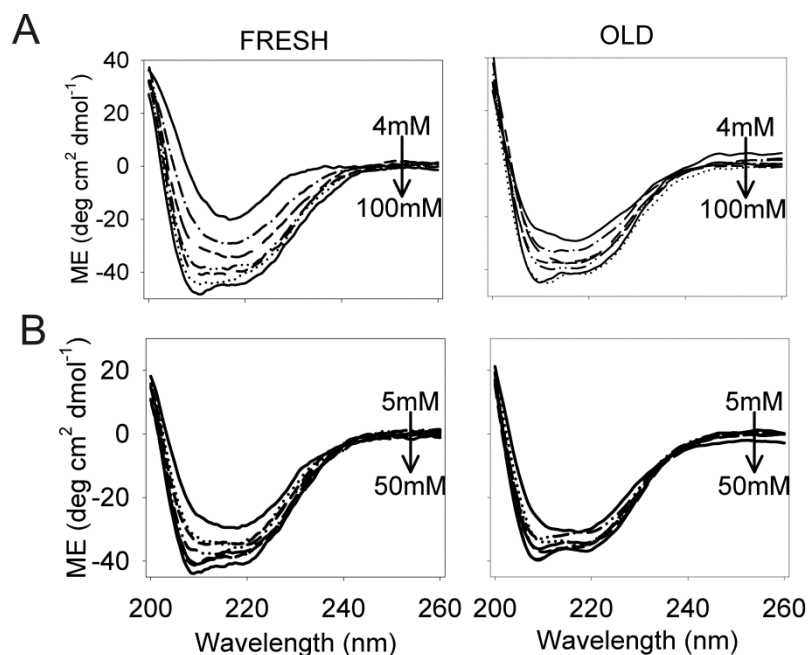
Figure S9. TM1 does not form amyloids or aggregates upon storage. Comparison of CD profiles of freshly prepared **TM1** in LDAO (A) and DPC (B) with peptide samples stored for 2.5 months at 4°C. CD profiles obtained in both lipids for old samples are comparable to that of freshly refolded peptide, indicating that **TM1** does not exhibit aggregation with time. This is singularly interesting for low LPR samples, wherein a CD spectrum corresponding to a β-sheet structure is obtained, and it can be anticipated that the 'sticky edges' of the strand segments would nucleate aggregation process. However, no aggregation is observable for **TM1** in our experiments. ME (molar ellipticity) values are factored by 10^4.
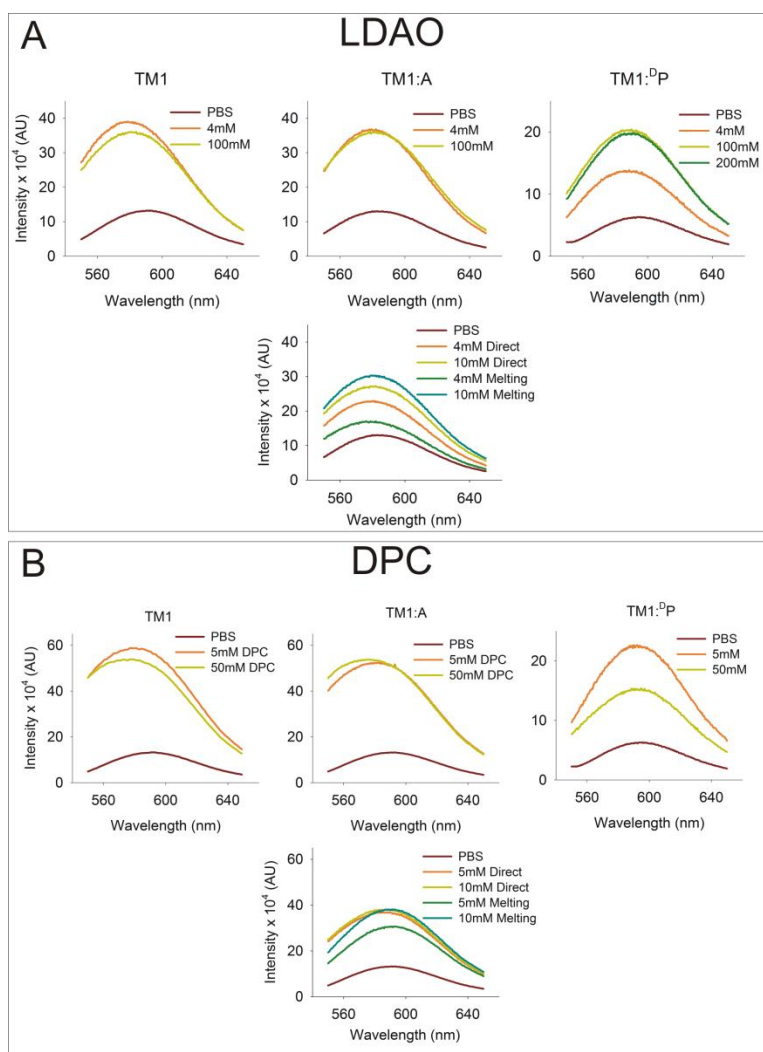
Figure S10. SYPRO® orange fluorescence as a probe of peptide folding in LDAO (A) and DPC (B). SYPRO® orange is quenched in aqueous media but exhibits an increase in fluorescence intensity upon binding to hydrophobic regions of proteins and peptides. SYPRO® orange penetrates LDAO micelles (A) and can bind to the transmembrane segment of **TM1** (left, top) and **TM1:A** (middle, top) or **TM1:^{D}P** (right, top), whereas the aggregated peptide in buffer (PBS) has a minimally exposed hydrophobic surface, thereby resulting in marginal SYPRO® orange fluorescence. This experiment, in conjunction with ThT assay, ratifies that the β-sheet conformation adopted by **TM1** in 4mM LDAO is embedded within LDAO micelles. The additional graph for **TM1:A** (bottom) shows the SYPRO® orange assays carried out on samples prepared by the direct addition of peptide to 4mM or 10mM LDAO. This data is compared with the 'β-sheet' structures observed after thermal melt experiments in the same lipid concentrations. The highest loss in SYPRO® orange fluorescence is observed in the case of **TM1:A** in 4mM LDAO subjected to thermal denaturation, suggesting the presence of aggregated peptide in low LPRs. However, examination of the anisotropy and lifetime data (described later) for **TM1:A** directly refolded in 4mM or 10mM LDAO indicates that the values are midway between the aggregated peptide in buffer and the refolded peptide in lipid. This suggests that directly refolded **TM1:A** forms tightly associated ordered β-sheet structures that are different from the aggregated form seen for the peptide in the absence of any lipid. A similar result is obtained for DPC (B).

```
PGKIRETLYYVGTLVILGIALIWGGIDA----PG     1-2
KIPGRETLYYVGTLVILGIALIWGGIDA----PG     3-4
KIREPGTLYYVGTLVILGIALIWGGIDA----PG     5-6
KIRETLPGYYVGTLVILGIALIWGGIDA----PG     7-8
KIRETLYYPGVGTLVILGIALIWGGIDA----PG     9-10
KIRETLYYVGPGTLVILGIALIWGGIDA----PG     11-12
KIRETLYYVGTLPGVILGIALIWGGIDA----PG     13-14
KIRETLYYVGTLVIPGLGIALIWGGIDA----PG     15-16
KIRETLYYVGTLVILGPGIALIWGGIDA----PG     17-18
KIRETLYYVGTLVILGIAPGLIWGGIDA----PG     19-20
KIRETLYYVGTLVILGIALIPGWGGIDA----PG     21-22
KIRETLYYVGTLVILGIALIWGPGGIDA----PG     23-24
KIRETLYYVGTLVILGIALIWGGIPGDA----PG     25-26
KIRETLYYVGTLVILGIALIWGGIDAPG----PG     27-28
```

PG $^{14-15}$

AA $^{14-15}$

```
KIRETLYYVGTLVPGILGIALIWGGIDA----PG    14-15
KIRETLYYVGTLVAAILGIALIWGGIDA----AA    14-15
```

Figure S11. I-TASSER simulation results of systematic PG substitution in TM1 sequence. A PG 'walk' was carried out for TM1 sequence (listed above) and the best structure calculated is shown as a ribbon diagram. Note that loss in helical structure is observed in cases wherein the PG segment is located towards the middle of the peptide sequence.
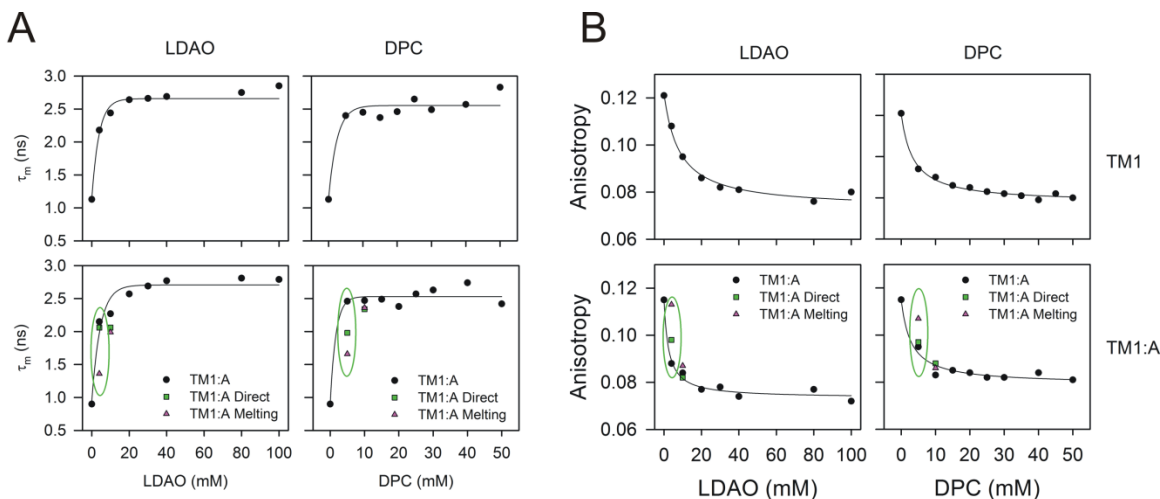
Figure S12. Change in Trp fluorescence lifetime (A) and anisotropy (B) with increase in LDAO or DPC concentrations. In all graphs, the 0mM data corresponds to data recorded for the peptide in buffer. Fits to an exponential function are shown, only to highlight the increase in lifetime values for the refolded peptide. Comparable profiles obtained for both **TM1** and **TM1:A** indicates that although **TM1** adopts a non-helical structure in low LPR, the local Trp environment is similar to the Trp residue of **TM1:A**, which remains helical in all LPRs. Additionally, in the case of **TM1:A**, data recorded for peptides directly refolded in 4mM or 10mM LDAO (Direct; green squares), and samples subjected to thermal denaturation under the same LDAO concentrations (Melting; pink triangles), are also included (lower panels). Note how samples refolded directly in LDAO or those prepared by dilution show similar lifetime or anisotropy values. However, after thermal denaturation, the lifetime values (A) and anisotropy data (B) obtained for the 4mM samples (lower left panel in both A and B) or 5mM DPC samples (lower right panel in both A and B) are closer to the aggregated peptide (encircled). Thermal denaturation therefore causes irreversible conformational conversion in **TM1:A**, leading to possible formation of tightly associated ordered β-sheets that can no longer be dissociated by lipid addition. Similar observations have been made earlier for Ala-containing peptide helices in lipid environments, using circular dichroism experiments.[8]
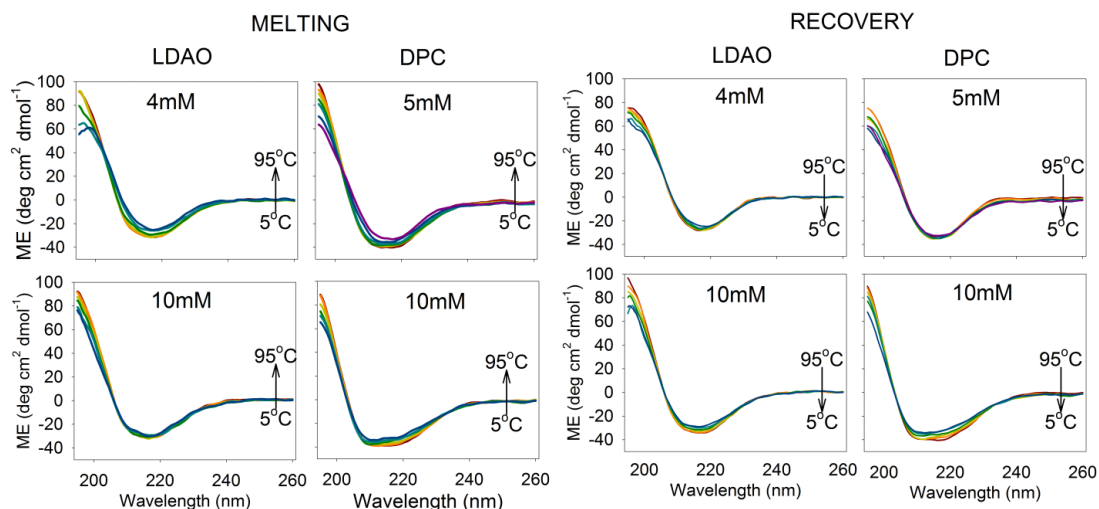
Figure S13. Comparison of denaturation and recovery profiles of **TM1:A** prepared by direct refolding of the peptide into various LDAO and DPC concentrations. Unlike CD profiles for **TM1:A** observed in Figure S5 in 4mM and 10mM LDAO, as well as 5mM and 10mM DPC shown in Figure S6, direct refolding of this peptide in low lipid concentrations results in adoption of a β-sheet structure under these conditions. When these samples are subjected to thermal denaturation, they undergo irreversible β-sheet formation and possible aggregation. As a result, no recovery in CD profiles is observed for **TM1:A** under these conditions, unlike that of **TM1** under similar conditions. Additionally, while **TM1** shows a conformational switch upon dilution (see Figure 2D of the main text), no such behavior is exhibited by **TM1:A** in low LDAO and DPC concentrations. ME (molar ellipticity) values in all spectra shown here are factored by 10^4.
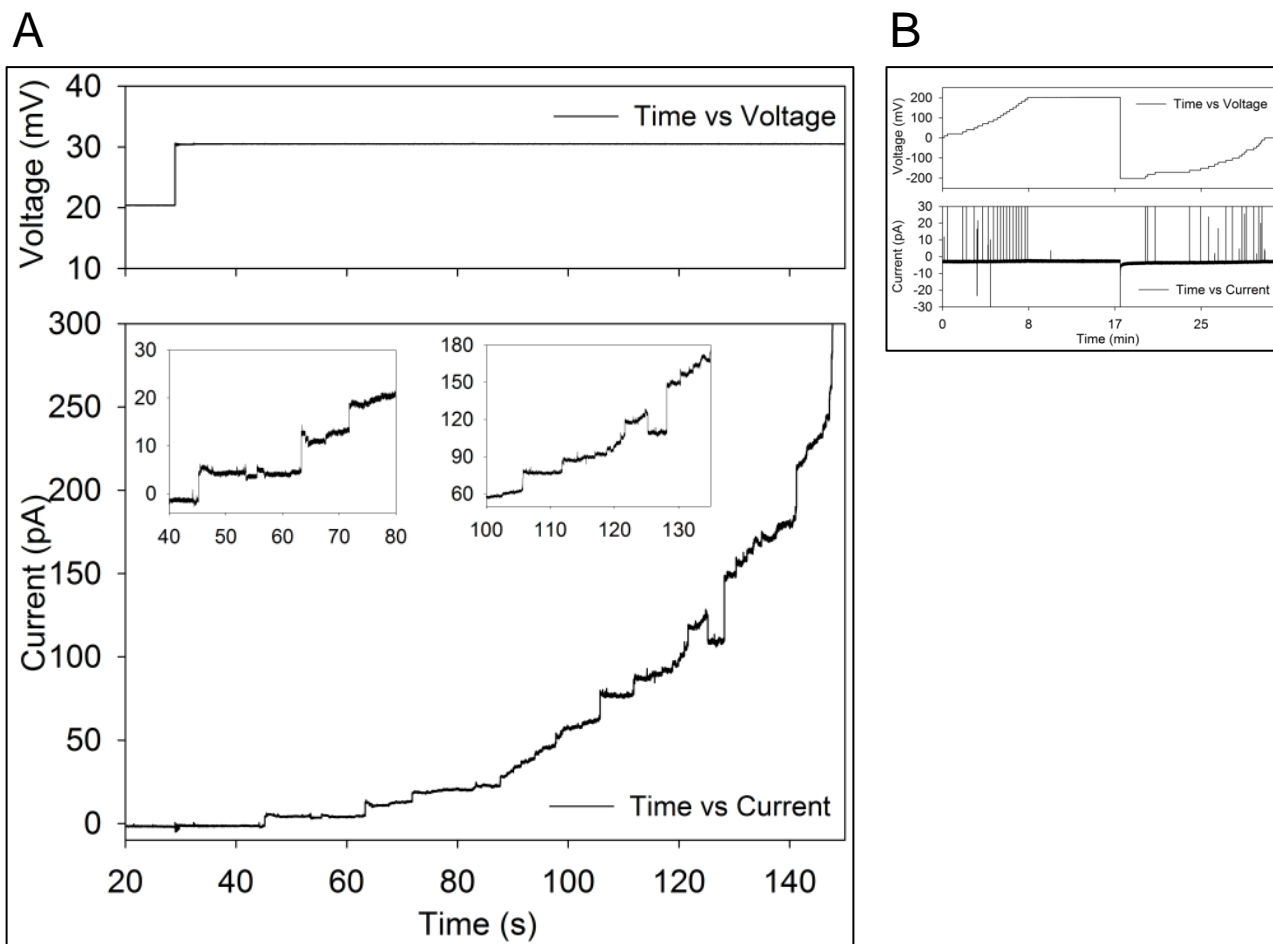
Figure S14. Black lipid membrane (BLM) experiments of **TM1** refolded in LDAO micelles and inserted in DPhPC membranes. (A) Bilayers formed across a 150μm pore in a Delrin cup were monitored for stability for 30min, after which **TM1** was added to the *cis* side, while the membrane was held at 0mV. Shown here is a representative trace of one such recordings. Immediately after peptide addition, the applied membrane potential was increased to a fixed voltage of +10mV. This was then stepped-up to +20mV and then +30mV. At this voltage, pore formation was observed within a few seconds, as deduced from the observed steps of 5pA current (inset on the left in (A)). We speculate that further peptide assembly and the formation of larger pores leads to a rapid increase in the observed signal (over 200pA) and finally membrane disruption within 1min. Also shown for comparison in (B) is a representative recording obtained when no peptide was added to the set-up, to demonstrate the stability of the formed membrane in the absence of any peptide. The voltage in this case was ramped from 0mV to +200mV to -200mV and brought back to 0mV. No current was observed across the membrane. The spikes in this recording correspond to each step in the voltage. Similar experiments were carried out for **TM1:A** and **TM1:^{D}P**. Under identical experimental conditions, we could not obtain consistent peptide insertion, particularly in **TM1:^{D}P**, and/or channel formation for either samples. We are tempted to speculate that the former observation is likely the effect of the ability of **TM1:^{D}P** to effectively insert in DPhPC membranes, suggesting that a helical structure is better able to penetrate a lipid bilayer. Once the membrane insertion event is accomplished, it is likely that the structural conversion brings about pore formation. This deduction essentially emphasizes the importance of a Pro-Gly segment for pore-forming activity.

SUPPLEMENTARY TABLE

Table S1. Summary of observed anisotropy values monitored using the single Trp residue of **TM1** and **TM1:A** in LDAO and DPC.

LDAO (mM)	Anisotropy			DPC (mM)	Anisotropy		
	TM1	TM1:A	TM1:^{D}P		TM1	TM1:1	TM1:^{D}P
0	0.121	0.115	0.130	0	0.121	0.115	0.130
4	0.108	0.088	0.106	5	0.094	0.095	0.108
4[#]	-[a]	0.098	-[a]	5[#]	-[a]	0.097	-[a]
4[$]	-[a]	0.113	-[a]	5[$]	-[a]	0.107	-[a]
10	0.095	0.084	0.101	10	0.090	0.083	0.103
10[#]	-[a]	0.082	-[a]	10[#]	-[a]	0.088	-[a]
10[$]	-[a]	0.087	-[a]	10[$]	-[a]	0.086	-[a]
20	0.086	0.077	0.099	15	0.086	0.085	0.102
30	0.082	0.078	0.098	20	0.085	0.084	0.099
40	0.081	0.074	0.096	25	0.083	0.082	0.098
80	0.076	0.077	0.093	30	0.082	0.082	0.096
100	0.080	0.072	0.092	35	0.081	-[a]	-[a]
				40	0.079	0.084	0.092
				45	0.082	-[a]	-[a]
				50	0.080	0.081	0.087

[a]Not determined. [#]Peptide was refolded directly into the respective lipid and recorded before thermal denaturation. [$]Sample prepared by dilution from stock solutions was recorded after subjecting to thermal denaturation.

REFERENCES FOR SUPPLEMENTARY INFORMATION

1. (a) C. Wu, M. Biancalana, S. Koide and J. E. Shea, *J. Mol. Biol.*, 2009, **394**, 627-633; (b) M. Biancalana and S. Koide, *Biochim. Biophys. Acta*, 2010, **1804**, 1405-1412.
2. (a) F. H. Niesen, H. Berglund and M. Vedadi, *Nat. Protoc.*, 2007, **2**, 2212-2221; (b) J. J. Lavinder, S. B. Hari, B. J. Sullivan and T. J. Magliery, *J. Am. Chem. Soc.*, 2009, **131**, 3794-3795.
3. A. Roy, A. Kucukural and Y. Zhang, *Nat. Protoc.*, 2010, **5**, 725-738.
4. L. Schrodinger, *The PyMOL Molecular Graphics System, Version 1.5.0.5*, 2010.
5. A. Krogh, B. Larsson, G. von Heijne and E. L. Sonnhammer, *J. Mol. Biol.*, 2001, **305**, 567-580.
6. E. L. Ulrich, H. Akutsu, J. F. Doreleijers, Y. Harano, Y. E. Ioannidis, J. Lin, M. Livny, S. Mading, D. Maziuk, Z. Miller, E. Nakatani, C. F. Schulte, D. E. Tolmie, R. Kent Wenger, H. Yao and J. L. Markley, *Nucleic Acids Res.*, 2008, **36**, D402-408.
7. S. R. Maurya, D. Chaturvedi and R. Mahalakshmi, *Sci. Rep.*, 2013, **3**, 1989.
8. S. C. Li, N. K. Goto, K. A. Williams and C. M. Deber, *Proc. Natl. Acad. Sci. U. S. A.*, 1996, **93**, 6676-6681.